IDENTIFICATION OF A NOVEL COHESIVE ZONE LAW IN AN INTERFACE FINITE ELEMENT FOR SIMULATING DELAMINATION WITH R-CURVE EFFECTS

S.M. Jensen[1], M.J. Martos, B.L.V. Bak, E. Lindgaard

Department of Materials and Production, Aalborg University, Fibigerstraede 16, Aalborg DK-9220, Denmark.
[1]E-mail: smj@mp.aau.dk

Keywords: Delamination, cohesive zone modelling, inverse parameter identification, optimization, large-scale bridging.

Abstract
This paper is concerned with modelling of quasi-static delamination in fibrous laminated composites exhibiting R-curve effects. The objective of the work is two-fold; initially a novel cohesive law is formulated which enables R-curve modelling over conventional cohesive laws. Secondly, a methodology for identification of fracture related parameters of the cohesive law is developed. The outcome are tested for simulating quasi-static delamination in glass-epoxy specimens loaded in pure mode I. The results show excellent agreement with experimental measurements, and the necessity of the novel cohesive law is evident by comparison with results obtained from conventional cohesive laws.

1. Introduction

Composite materials are widely used in thin-walled structures for high performance applications, e.g. aeronautics, wind turbine blades, and sports equipment. This is mainly due to their tailorable properties and high in-plane specific strength and stiffness. Delamination is one of the most damaging and frequently occurring failure types in engineering composite structures due to the relatively weak interface strength of a laminate. Peel stresses near free edges of a laminate or manufacturing defects etc., multiply the potential sites for delamination initiation. Subsequent delamination propagation, either static of fatigue-driven, can cause loss of structural integrity and catastrophic failure. Cohesive zone modelling is an increasingly popular and efficient tool for assessment of delamination initiation and propagation in laminated composites. The approach is specially suited in the framework of finite element analysis in combination with interface elements to model a delamination path, across which cohesive tractions relate to interfacial separations through cohesive laws. However, the quality and accuracy of current models depend heavily on the complexity of the material behavior involved in the fracture process. Especially R-curve effects, originating from large-scale fiber bridging in the wake of the crack tip, are difficult to represent using current cohesive zone models. This is due to inherent limitations in the shape of the cohesive law.

A first objective of the present paper is to develop a constitutive model of an interface finite element which enables R-curve modelling. In essence this requires that the crack interfaces can represent failure mechanisms on multiple scales within the fracture process zone. This is accomplished by adding more freedom to the shape of the cohesive law. Conventional cohesive laws are pragmatic in nature and seek simple traction-separation relations, e.g. bilinear or exponential, to represent the most essential physical properties acquired from conventional fracture mechanical tests and strength tests. However, such cohesive laws are far from adequate to model R-curve effects due to fiber bridging. In the open literature, researchers have published trilinear cohesive laws, as a simple extension of the bilinear relation, to achieve R-curve modelling. Although the trilinear cohesive law enables simulation of increasing fracture resistance as the crack evolves, the simulated response is still in poor agreement with the experimental findings of this paper. A novel generalized mixed-mode multilinear cohesive law consisting of an arbitrary number of line segments is proposed for modelling R-curve effects.

The cohesive law is implemented as a user-defined interface element in the commercial finite element program ANSYS Mechanical for implicit finite element analysis. Its application is demonstrated by simulating delamination in glass-epoxy double cantilever beam (DCB) specimens in pure mode I loading.

A second objective of the paper is devoted to material characterization. Given a framework that enables simulation of R-curve effects, as the multilinear cohesive law, one needs a tool for efficient and reliable identification of its properties. A methodology for characterization of multilinear cohesive laws is proposed. The methodology relies on inverse modelling of a physical experiment, and determine the cohesive law by minimization of a residual in terms of global structural responses using mathematical programming techniques. The motivation for a multilinear cohesive law is emphasized by comparison with the responses obtained using conventional bi- and trilinear cohesive laws.

2. Generalized Mixed-mode Multilinear Cohesive Law

The first objective of this work is to establish a cohesive zone model in a finite element framework that enables R-curve modelling. This is accomplished by proposing a novel constitutive formulation of existing cohesive zone models. The finite element implementation extends the interface element formulation proposed in [1,2], which contains a bilinear cohesive law for simulating delamination under mixed-mode loading. The constitutive model of the interface element is enriched by adding an arbitrary number of line segments to the cohesive law, which proves efficient to model R-curve effects. This work is only concerned with constitutive modelling, and no changes are done to the original kinematics. A thorough description of the constitutive model is available in [3]. This paper provides an outline and demonstrates the applicability of the cohesive zone model proposed.

The cohesive zone model is formulated in the framework of damage mechanics. A secant constitutive equation computes cohesive tractions, τ_i, for any value of the interfacial separation, Δ_i, and the damage state according to Eq. (1).

$$\tau_i = (1 - d)\delta_{ij} K \Delta_j - d\delta_{ij} K \delta_{3j} \langle -\Delta_3 \rangle \tag{1}$$

The cohesive law introduces a damage criterion to control degradation of the interfacial stiffness through a damage variable, d, and irreversibility of dissipated energy. The damage variable is a monotonically increasing scalar; it equals zero for pristine material and unity upon full damage. The evolution of the damage parameter is controlled by an equivalent one-dimensional cohesive law, which relates the separation norm, λ, and the equivalent one-dimensional cohesive traction, $\bar{\sigma}$:

$$\lambda = \sqrt{\Delta_s^2 + \langle \Delta_3 \rangle^2} \qquad \Delta_s = \sqrt{\Delta_1^2 + \Delta_2^2} \qquad \bar{\sigma} = K(1 - d)\lambda \tag{2}$$

In this work, the shape of the cohesive law is defined as a piecewise linear relation consisting of an arbitrary number of segments, i.e. a multilinear cohesive law. Considering the equivalent one-dimensional multilinear cohesive law in Fig. 1; the end-point coordinates, $(\bar{\delta}^{(i)}, \bar{\sigma}^{(i)})$, of the line segments determine the shape of the equivalent one-dimensional cohesive law, and is referred to as the mixed-mode cohesive zone variables. These variables are in general mode dependent and for a given instant of mixed-mode loading, these are determined by interpolation of pure mode I and pure shear mode cohesive laws, which can be experimentally measured. In that sense the cohesive zone variables of pure mode cohesive laws act as material properties of the laminate interface.

Due to the simple shape of conventional cohesive laws, e.g. bilinear, only a few cohesive zone variables are sufficient to uniquely define the shape. For a bilinear cohesive law, the mixed-mode cohesive zone variables can be interpolated from a mode dependent strength- and propagation criterion, together with a suitable measure of the degree of mode mixity. However, due to the large number of cohesive zone variables in a general multilinear cohesive law, the conventional use of such criteria is inadequate.

Given a total of 2n mixed-mode cohesive zone variables of the equivalent one-dimensional multilinear cohesive law, the same number of interpolation formulas are requested. In this work, every n'th mixed-mode traction variable is interpolated according to Eq. (3). The equation includes quadratic stress interaction and a B parameter which quantifies the instantaneous degree of mode mixity by a local and kinematic measure $\beta = \Delta_s/(\Delta_s + \langle\Delta_3\rangle)$.

$$\left(\bar{\sigma}^{(i)}\right)^2 = \left(\sigma_3^{(i)}\right)^2 + \left[\left(\sigma_s^{(i)}\right)^2 - \left(\sigma_3^{(i)}\right)^2\right] B^{\xi} \qquad \text{where} \qquad B = \frac{\beta^2}{1+2\beta^2-2\beta} \tag{3}$$

wherein ξ is an experimental curve fitting exponent. The mixed-mode separation variables are interpolated such that the resulting equivalent one-dimensional cohesive law is energy consistent with the modified BK-criterion in Eq. (4) [1,4]. The exponent η is a curve fitting exponent.

$$G_c = G_c^I + \left(G_c^s - G_c^I\right) B^{\eta} \tag{4}$$

Given the *n* mixed-mode separation variables to be determined, a total of *n-1* equations are derived from the modified BK-criterion. This is accomplished by splitting the total area under the cohesive law, i.e. the critical energy release rate [5], into *n* subintervals of every two consecutive separation variables $[\bar{\delta}^{(i-1)}; \bar{\delta}^{(i)}]$. In this approach, the modified BK-criterion interpolates subparts of the total fracture energy piecewise, as illustrated in Fig. 2 by the shaded areas. This approach provides *n-1* equations to determine $\bar{\delta}^{(i)}$ for *i=2…n*. The first mixed-mode separation variable, $\bar{\delta}^{(1)}$, are defined from the fixed penalty stiffness, K=10^5 N/mm^3, and the onset traction $\bar{\sigma}^{(1)}$.

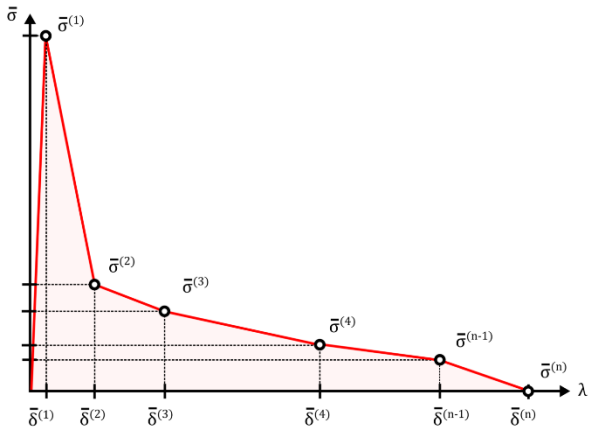

Fig. 1: One-dimensional equivalent multilinear cohesive law. Here shown with 6 line segments.

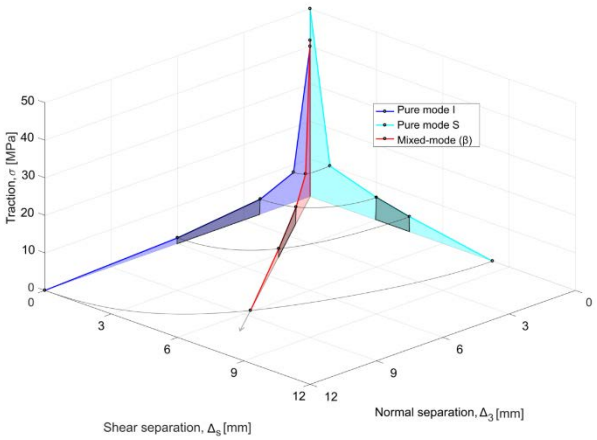

Fig. 2: Equivalent one-dimensional cohesive law and interpolation of pure mode cohesive laws.

3. Inverse parameter identification

As a second objective, a methodology for characterization of the cohesive zone variables of the multilinear cohesive law is proposed. This objective is covered in [6] in greater detail. This paper focus on a demonstration of the methodology. The methodology relies on inverse parameter identification by simulating a physical experiment using a parametric finite element model. Cohesive zone variables are then obtained by minimization of a least squares formulation of simulated and experimental responses. The overall procedure is illustrated in a flowchart in Fig. 3.

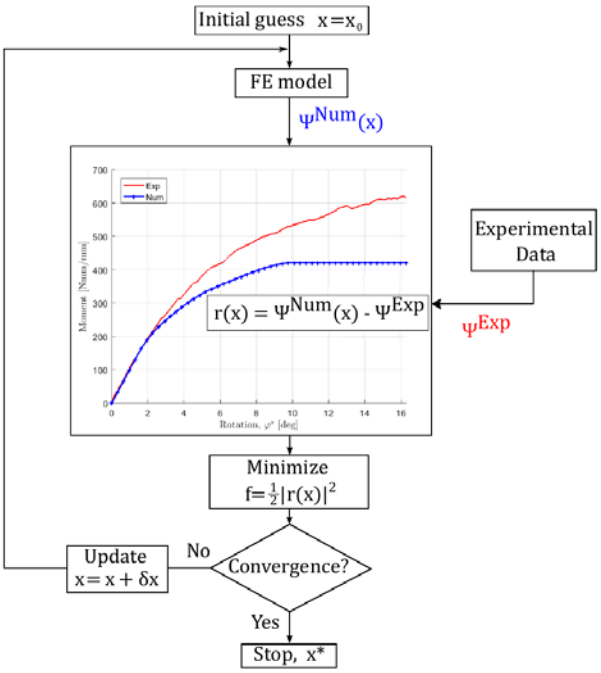

Fig. 3: Flowchart of the inverse parameter identification procedure.

The methodology defines a residiual, $\mathbf{r}(\mathbf{x})$, between measures of the global structural response in the experiment, $\mathbf{\Psi}^{\mathbf{Exp}}$, and the finite element model, $\mathbf{\Psi}^{\mathbf{Num}}(\mathbf{x})$. The size of $\mathbf{r}(\mathbf{x})$ depends on the extent and information in $\mathbf{\Psi}^{\mathbf{Exp}}$ and $\mathbf{\Psi}^{\mathbf{Num}}(\mathbf{x})$. The array $\mathbf{x}$ includes the cohesive zone variables to be determined. The objective function, $f(\mathbf{x})$, is formulated as a least squares formulation in terms of $\mathbf{r}(\mathbf{x})$ and the optimization problem is defined according to Eq. (5).

$$\underset{\mathbf{x}}{\text{MIN}}\, f(\mathbf{x}) = \frac{1}{2}|\mathbf{r}(\mathbf{x})|^2 \quad \text{subjected to} \qquad (5)$$
$$g_j(\mathbf{x}) \leq 0 \;\; \text{for } j = 1 \ldots k$$

Where $g_j(\mathbf{x})$ is a linear inequality constraint function, which ensures the cohesive law is monotonically softening. The optimization problem is solved using a gradient-based interior-point algorithm available in MATLAB [7]. This algorithm allows for inclusion of second-order information. The least squares formulation is convenient for this purpose, as the Hessian can be readily estimated from the Jacobian.

The generality of the framework allows any variables of the cohesive law to be included in $\mathbf{x}$. In this work, it is chosen to pre-define the distribution of separation variables such that only traction variables are included in $\mathbf{x}$. This choice adds little restrictions to the shape of the multilinear cohesive law provided the number of line segments included is sufficiently large. Additionally, it is both convenient and computationally reasonable to have variables of equal order of magnitude, units, and physical interpretation for improved scaling of the optimization problem and ease of defining the linear inequality constraint functions $g_j(\mathbf{x})$. The first and last traction variables are excluded from the optimization problem. The onset traction is set equal to 80% of the out-of-plane strength of the laminate, while the last traction value is identically zero. Following this approach a multilinear cohesive law of *n* line segments includes a total of *n-2* design variables in $\mathbf{x}$.

The methodology is demonstrated by characterization of a pure mode I multilinear cohesive law consisting of 15 segments. Given the discussion above, the variables to be included in $\mathbf{x}$ appears in Tab. 1.

i	1	2	3	4	5	6	7	8	9	10	11	12	13	14	15
$\delta_3^{(i)}$ [mm]	$\sigma_3^{(1)}/K$	0.01	0.02	0.03	0.04	0.05	0.06	0.08	0.10	0.20	0.50	1.00	3.00	5.00	9.00
$\sigma_3^{(i)}$[MPa]	30	x_1	x_2	x_3	x_4	x_5	x_6	x_7	x_8	x_9	x_{10}	x_{11}	x_{12}	x_{13}	0

Tab. 1: Overview of cohesive zone variables and entities of **x** for a pure mode I experiment and a 15-segmented cohesive law.

4. Demonstration of identification methodology

The methodology is demonstrated by characterizing a multilinear cohesive law for a uni-directional glass fiber-epoxy laminated composite specimen. The specimen under consideration is a double cantilever beam (DCB) specimen subjected to quasi-static pure mode I bending loading. The experimental data is obtained in [8], which the reader is refered to for further information. The experimental setup is shown in Fig. 4. The experimental output is measurements of the applied force couple, M, versus the angle of rotation, θ, at the crack mouth of the DCB specimen. The output is shown in Fig. 5.

A parametric finite element model similar to that of the experiment is constructed in ANSYS Mechanical and used for the inverse modelling. The finite element model is shown in Fig. 6. The bulk material is modelled using eight-noded linear solid elements (SOLID185) with enhanced assumed strain. The path of delamination is pre-defined along the interface of the DCB arms at y=0. The interface is modelled using the user-defined interface element with the multilinear cohesive law. Rotational degrees of freedom are assigned to the end faces of the upper and lower DCB arms through multi-point constraints. This allows one to have a displacement controlled model by introducing the load as prescribed angles of rotation about the z-axis, as illustrated in Fig. 6. The finite element model is solved using a displacement-controlled Newton-Raphson solver with a line search procedure and an automatic pseudo time stepping algorithm.

The objective function is formulated in terms of the residual of global structural responses. In this demonstration, the residual, **r**(**x**), contains 60 entities, which quantify pointwise differences in the force couple at 60 pre-defined load steps. The load steps are equally distributed along the θ-axis in Fig. 5.

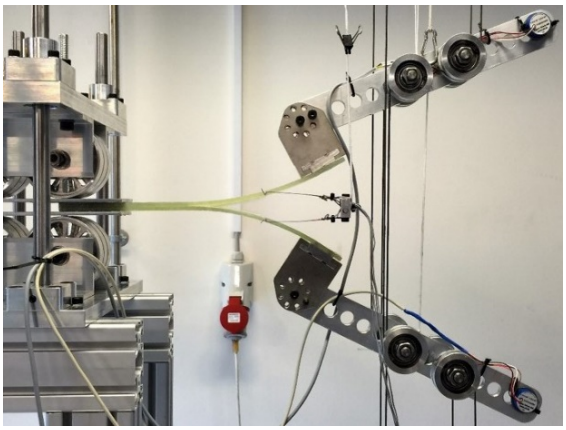

Fig. 4: Experimental setup. Inclinometers measure angle of rotation at the crack mouth, and the applied force couple is applied through a wire-pulley system connected to a tensile testing machine.

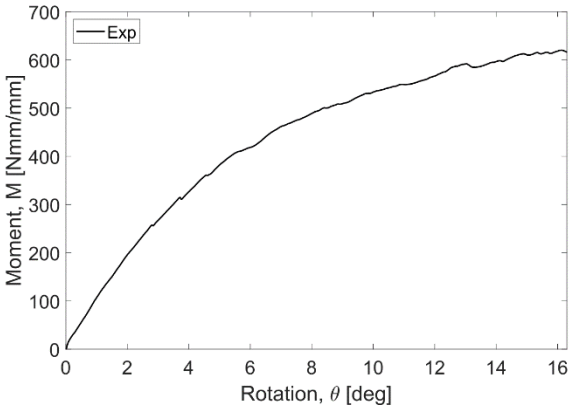

Fig. 5: Global structural response from [8].

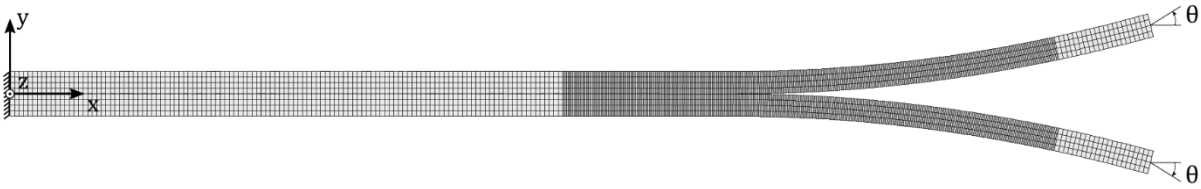

Fig. 6: Finite element model. Equal and opposite angles of rotation are prescribed at the end faces of the DCB arms.

5. Results

The methodology starts from an initial guess. Four distinct initial guesses have been tested to assess the robustness of the methodology and issues related to convexity of design space and local minima. The initial guesses are shown in Fig. 8 and the associated structural response is shown in Fig. 9. The plots of the initial guesses are split into two parts of different axis-scales for illustration purposes. The methodology progresses with the settings described in section 3, and converges to the cohesive laws shown in Fig. 10 within 79-99 iterations. The cohesive laws are completely identical in the right part of Fig. 10, which dominates the bridging consititutive behavior. The minor differences observed in the left part of Fig. 10 has a maximum deviation of 0.10 MPa, and are irrelevant for the structural response. All solutions agree in terms of the critical energy release rate, $G_c = 2.3\text{kJ/m}^2$. The structural responses associated with the converged solutions are included in Fig. 11. The figure shows an execellent agreement with the experimental response, and no notable differences are seen in the simulated responses. Lastly, the structural response of the multilinear cohesive law is compared to the conventional bi- and trilinear cohesive laws. The bi- and trilinear cohesive laws are characterized using the proposed methodology described in section 3. The cohesive laws and the structural responses are shown in Fig. 12 and 13, respectively. The need for a multilinear cohesive law is clear from the figure. The bilinear cohesive law completely lacks the ability to model R-curve effects, whereas limited accuracy is obtained when using the trilinear cohesive law.

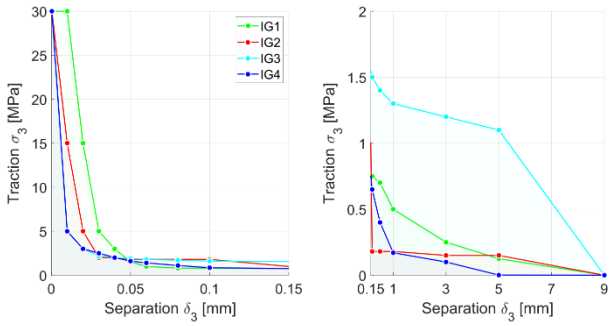

Fig. 8: Initial guesses of cohesive laws, IG1-4.

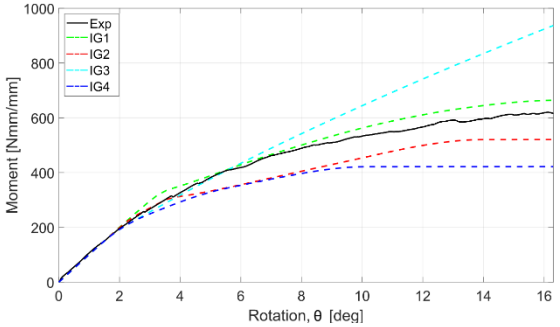

Fig. 9: Structural response associated IG1-4.

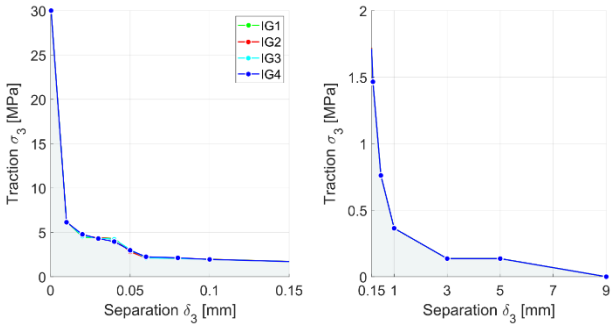

Fig. 10: Converged solutions for IG1-4.

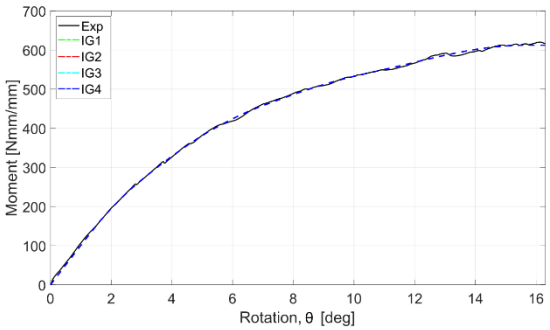

Fig. 11: Structural response associated with solutions.

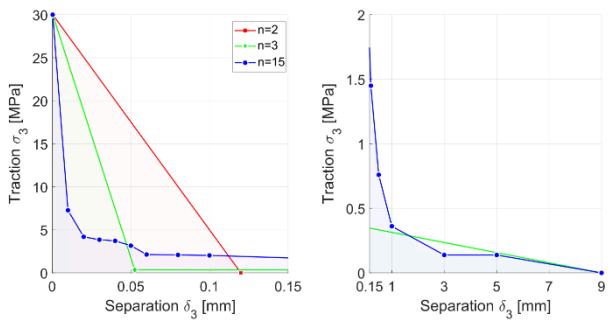

Fig. 12: Multilinear and conventional cohesive laws.

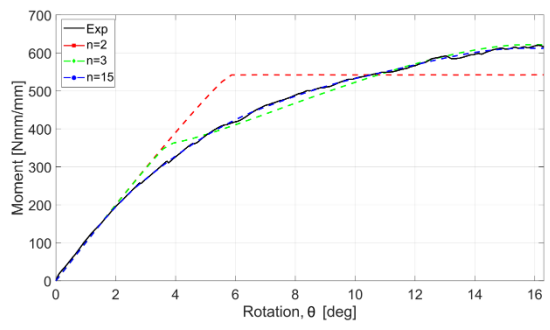

Fig. 13: Structural response associated Fig. 12.

6. Conclusion

A mixed-mode multilinear cohesive law is proposed for simulating quasi-static delamination in fibrous laminated composites with R-curve behaviour. The multilinear formulation adds freedom to the shape of the cohesive law which proves efficient to model R-curve effects over conventional bi- and trilinear cohesive laws. Secondly, a methodology for identification of fracture related parameters of the multilinear cohesive law is developed. The methodology uses inverse parametric finite element modelling and mathematical programming techniques to characterize the cohesive law. The work is demonstrated by characterizing a 15-segmented multilinear cohesive law of a uni-directional glass fiber-epoxy laminated composite specimen in pure mode I quasi-static loading. The methodology proves robust and accurate in determining the cohesive law. The paper outlines and demonstrates the applicability of the cohesive zone model and identification methodology proposed in [3,6], to which the reader is refered to for more information.

References

[1]: A. Turon, P. Camanho, J. Costa, C. Davila. A damage model for the simulation of delamination in advanced composite under variable-mode loading. *Mechanics of Materials* 38:1072-1089, 2006.
[2]: E. Lindgaard, B.L.V. Bak, J. Glud, J. Sjølund, E. Christensen. A user programmed cohesive zone finite element for ansys mechanical. *Engineering Fracture Mechanics*, 180:229-239, 2017.
[3]: S.M. Jensen, M.J. Martos, B.L.V. Bak, E. Lindgaard. Formulation of a mixed-mode multilinear cohesive zone law in an interface finite element for modelling delamination with R-curve effects. (*Submitted for review)*.
[4]: M.L. Benezeggagh, M. Kenane. Measurement of mixed-mode delamination fracture toughness of unidirectional glass/epoxy composites with mixed mode bending apparatus. *Composites Science and Technology*, 56:439-449, 1995.
[5]: J. R. Rice. A path independent integral and the approximate analysis of strain concentration by notches and cracks. *Journal of Applied Mechanics*, 35:379-386, 1968.
[6]: M.J. Martos, S.M.Jensen, E. Lindgaard, B.L.V. Bak. Inverse parameter identification of n-segmented multilinear cohesive laws. (*Submitted for review)*
[7]: MATLAB - Image Processing Toolbox user's guide, MathWorks, R2017b.

[8]: Experimental characterization of delamination of off-axis GFRP laminates during mode I loading. (*Submitted for review*)